DOT/FAA/AR-04/40,P2

Office of Aviation Research
Washington, D.C. 20591

Explicit Finite Element Modeling of Multilayer Composite Fabric for Gas Turbine Engine Containment Systems

Part 2: Ballistic Impact Testing

November 2004

Final Report

This document is available to the U.S. public through the National Technical Information Service (NTIS), Springfield, Virginia 22161.

U.S. Department of Transportation
Federal Aviation Administration

NOTICE

Technical Report Documentation Page

1. Report No.	2. Government Accession No.	3. Recipient's Catalog No.
DOT/FAA/AR-04/40,P2		

4. Title and Subtitle	5. Report Date
EXPLICIT FINITE ELEMENT MODELING OF MULTILAYER COMPOSITE FABRIC FOR GAS TURBINE ENGINE CONTAINMENT SYSTEMS PART 2: BALLISTIC IMPACT TESTING	November 2004
	6. Performing Organization Code
7. Author(s)	8. Performing Organization Report No.
J. Michael Pereira and Duane M. Revilock	
9. Performing Organization Name and Address	10. Work Unit No. (TRAIS)
NASA Glenn Research Center 21000 Brookpark Road Cleveland, OH 44135	11. Contract or Grant No. 01-C-AW-ASU Subagreement 02-11
12. Sponsoring Agency Name and Address	13. Type of Report and Period Covered
U.S. Department of Transportation Federal Aviation Administration FAA William J. Hughes Technical Center Atlantic City International Airport, NJ 08405	Final Technical Report 8/2001 – 5/2003
	14. Sponsoring Agency Code ANE-100

15. Supplementary Notes

The FAA William J. Hughes Technical Center COTR was Donald Altobelli.

16. Abstract

Under the Federal Aviation Administration's Airworthiness Assurance Center of Excellence and the Aircraft Catastrophic Failure Prevention Program, National Aeronautics and Space Administration Glenn Research Center collaborated with Arizona State University, Honeywell Engines, Systems and Services, and SRI International to develop improved computational models for designing fabric-based engine containment systems. In the study described in this report, ballistic impact tests were conducted on layered dry fabric rings to provide impact response data for calibrating and verifying the improved numerical models. The impact energy absorption responses of two different fabrics, Kevlar 49® and Zylon AS®, in two different fabric architectures, were compared. It was found that for the same fabric architecture, under the given impact conditions, Zylon® was able to absorb almost three times the energy of the equivalent weight Kevlar®. This report provides data on projectile velocity, impact and residual energy, and fabric deformation for a number of different test condition

17. Key Words	18. Distribution Statement
Fan containment, Jet engine, Composite fabric, Ballistic impact, Zylon, Kevlar	This document is available to the public through the National Technical Information Service (NTIS) Springfield, Virginia 22161.

19. Security Classif. (of this report)	20. Security Classif. (of this page)	21. No. of Pages	22. Price
Unclassified	Unclassified	36	

Form DOT F1700.7 (8-72) Reproduction of completed page authorized

TABLE OF CONTENTS

LIST OF FIGURES

LIST OF TABLES

EXECUTIVE SUMMARY

Modeling a multilayer fabric composite for engine containment systems during a fan blade-out event has been a challenging task. Nonlinear transient (explicit) finite element analysis has the greatest potential of any numerical approach available to industry for analysis of these events. Significant research is still required to overcome difficulties with numerical stability, material modeling (pre- and postfailure), and standardizing modeling methods to achieve accurate simulation of the complex interactions between individual components during these high-speed events. The primary focus of this research was to develop the methodology for testing, modeling, and analyzing a typical fan blade-out event in a multilayer fiber fabric composite containment system. ABAQUS finite element code was used to verify the basic material model (prefailure state) developed through laboratory testing. LS-DYNA was the primary modeling tool used in the explicit finite element analysis of ballistic events.

During the Fourth Federal Aviation Administration (FAA) Uncontained Engine Debris Characterization Modeling and Mitigation Workshop (held in May 2000 at SRI International, Menlo Park, CA), a representative of Honeywell Engines, Systems & Services presented the capability of modeling complicated engine hub-burst and fan blade-out events. Predicting most of the event with high confidence was shown. At the same time, SRI presented their efforts on modeling the material characteristics within LS-DYNA and developing a new composite fiber material called Zylon® that appeared to be stronger, lighter, and more temperature-resistant than Kevlar®. Both parties showed interest in each other's work, and both agreed they could benefit from each other if collaborative mechanisms could be arranged. After the workshop, Honeywell and SRI contacted each other and began talks of a joint project. The FAA, National Aeronautics and Space Administration (NASA) Glenn Research Center (GRC), and Arizona State University (ASU) were later invited into the discussion, resulting in this FAA-funded research under the Aircraft Catastrophic Prevention Program and the Airworthiness Assurance Center of Excellence Program.

The goal of this research was to use the technical strengths of Honeywell, SRI, and the ASU for developing a robust explicit finite element analysis modeling methodology for the purposes mentioned above. Since the development of an experimental set of data to support the calibration of the finite element models is essential, various experimental methods to measure material and structural response of the fabrics were conducted. NASA GRC, under the NASA Aviation Safety Program, conducted a series of engine containment ring tests that were used for modeling in this program.

Each member of the team took a leadership role and developed a comprehensive report describing the details of the research task and the findings. The complete FAA report is comprised of the following four separate reports (parts 1 through 4).

- Part 1: Static Tests and Modeling by Arizona State University Department of Civil Engineering

- Part 2: Ballistic Testing by NASA Glenn Research Center

- Part 3: Material Model Development and Simulation of Experiments by SRI International

- Part 4: Model Simulation for Ballistic Tests, Engine Fan Blade-Out, and Generic Engine by Honeywell Engines, Systems & Services

Ballistic impact tests were conducted at NASA GRC on dry Kevlar 49® and Zylon AS® fabric specimens in a test configuration designed to simulate its application in a turbine engine fan containment system. This report (part 2 of 4) provides data on projectile velocity, impact and residual energy, and fabric deformation for a number of different test conditions.

A single-fabric architecture was used for the Kevlar® material and two different architectures were used for the Zylon®, one similar to the Kevlar and another significantly lighter. Twenty-five-cm (10-in.)-wide continuous strips of the fabric were wound around a steel ring with a diameter of 102 cm. The ring was placed in front of a 20-cm (7.9-in.)-diameter gas gun at a slight incline so that the projectile passed over the leading edge of the ring and impacted the fabric through a slot from the general direction of the center of the ring. The projectile was a flat piece of 304L stainless steel 10.2 cm (4.0 in.) long, 5.1 cm (2.0 in.) high, and 0.48 cm (0.188 in.) thick, with a mass of approximately 320 gm (0.7 lb). The projectile impacted the specimen edge on. Under these conditions, Zylon was able to absorb almost three times the energy of the equivalent weight Kevlar.

1. INTRODUCTION.

1.1 PURPOSE.

This research effort was undertaken as a direct result of discussions from the Fourth Federal Aviation Administration (FAA) Uncontained Debris Characterization Modeling and Mitigation Workshop (held in May 2000 at SRI International). A team effort between government, academia, and industry was seen as an excellent opportunity to transition fabric modeling and testing research that was being sponsored by the FAA Aircraft Catastrophic Failure Prevention Program and the National Aeronautics and Space Administration (NASA) Aviation Safety Program into commercial aircraft.

1.2 BACKGROUND.

International aviation regulatory bodies, such as the FAA in the United States and the Joint Aviation Authorities in Europe, require that in commercial jet engines a system must exist that will not allow any single compressor or turbine blade failure to perforate the engine case during engine operation [1]. They further require that jet engine manufacturers demonstrate, through a certification test, that the most critical blade be contained within the engine when a blade is released while the engine is running at full-rated thrust. The most critical compressor blade in the engine, in terms of maximum kinetic energy, is invariably the fan blade, and the system designed to prevent it from penetrating the engine is called the fan containment system.

There are two general types of fan containment systems, commonly referred to as hard-wall and soft-wall systems. Hard-wall systems consist of a relatively stiff section of the engine case that has sufficient strength to prevent perforation if impacted by a blade. Generally, there is relatively little deflection involved during impact with a hard-wall system. Soft-wall systems usually consist of a thin inner ring, surrounded by layers of dry fabric, most commonly Kevlar®. Between the inner ring and the fabric there is usually some structural material, such as honeycomb, to provide stiffness to the case. Energy absorption in soft-wall systems is accompanied by large deformation in the fabric.

The process of designing a containment system is based largely on empirical methods supported by impact testing of subscale components. However, there is strong motivation on the part of jet engine manufacturers to develop numerical models that can be used to help in the design process of fan containment systems, thereby reducing the cost of testing and increasing confidence and reliability in the design.

A number of research and commercial computer programs are available that can simulate the impact of a released fan blade on the case (a blade-out event). These are generally transient, explicit integration finite element codes [2 and 3]. The codes themselves are accurate and have been validated by years of use, but the constitutive, failure, and contact models are still the subject of active research. A large body of data and research studies exist with regard to high strain rate behavior impact response, and constitutive/failure models for metals [4, 5, and 6]. While there is data available in the literature on the impact response of fabrics [7, 8, and 9], and models have been developed to simulate fabric impact response [10, 11, and 12] the body of literature is much smaller than for metals. In addition, studies tend to focus on applications other than jet engines, such as body armor, and generally consider impacts involving a relatively small number of fabric layers.

This study was one of several being conducted by a FAA-sponsored Airworthiness Assurance Center of Excellence (AACE) team that included Arizona State University, Honeywell Engines, Systems & Services, SRI, and NASA Glenn Research Center. The aim of the AACE program was to develop improved computational tools for designing fabric-based engine containment systems. The objective of this particular study was to provide impact response data on fabric systems that would be used for calibrating and verifying the improved numerical models. A secondary objective was to compare the impact energy absorption response of two different fabrics, Kevlar and Zylon® in two different fabric architectures. The impact conditions were selected to be more representative of engine blade-out events than is typically seen in the literature, while keeping the test as simple and reproducible as possible.

2. METHODS.

The general experimental procedure used in this study involved conducting ballistic impact tests on layers of dry fabric. The impact energy was held constant, with the exception of a small number of tests, while the number of layers of fabric was varied. The fabric was wound around a circular fixture placed in front of a gas gun at a slight incline such that the projectile exited the gun barrel, passed over the leading edge of the ring, and impacted the fabric from the inside.

2.1 MATERIALS.

Fabrics, woven from two different fiber materials, Kevlar 49® and Zylon AS®, were tested. Kevlar is a material with a long history in impact applications, in general, and fan containment systems, in particular [13 and 14]. Zylon, sometimes referred to as PBO (poly-benzoxazole), has been under development more recently. A number of studies have shown that Zylon demonstrates superior performance over Kevlar under laboratory impact test conditions [15 and 16]. In this study, Kevlar was tested in a single-fabric architecture, while two-fabric architectures, were used for Zylon. The fiber and weave parameters of the materials used in this study are shown in table 1 [17].

TABLE 1. FABRIC PROPERTIES

		Zylon AS PBO		Kevlar-49 P-Aramid
		Light	Heavy	Standard
Volume density	(g/cm^3)	1.54	1.54	1.44
Yarn denier (measured)	(g/9km)	500	1500	1490
Yarn linear density	(mg/cm)	0.556	1.654	1.656
Yarn count	(yarns/in)	35 x 35	17 x 17	17 x 17
Yarn count	(yarns/cm)	13.8 x 13.8	6.7 x 6.7	6.7 x 6.7
Fabric ply thickness	(mm)	0.21	0.28	0.28
Fabric areal density	(g/cm^2)	0.01575	0.0223	0.02275
Degree of crimp warp yarns	(%)	3.1	2.2	1.1
Degree of crimp fill yarns	(%)	0.6	0.9	0.8

2.2 TEST CONFIGURATION.

The projectile used in the impact tests was a flat, rectangle-shaped piece of 304L stainless steel, 10.2 cm (4.0 in.) long, 5.1 cm (2.0 in.) high, and 0.48 cm (0.188 in.) thick (figure 1), with a mass of approximately 320 gm (0.7 lb). The front edge of the projectile was machined with a full radius. It exited the gun barrel in such a way that the long dimension of the projectile was in the direction of travel, the height dimension was vertical and the thickness dimension was side to side.

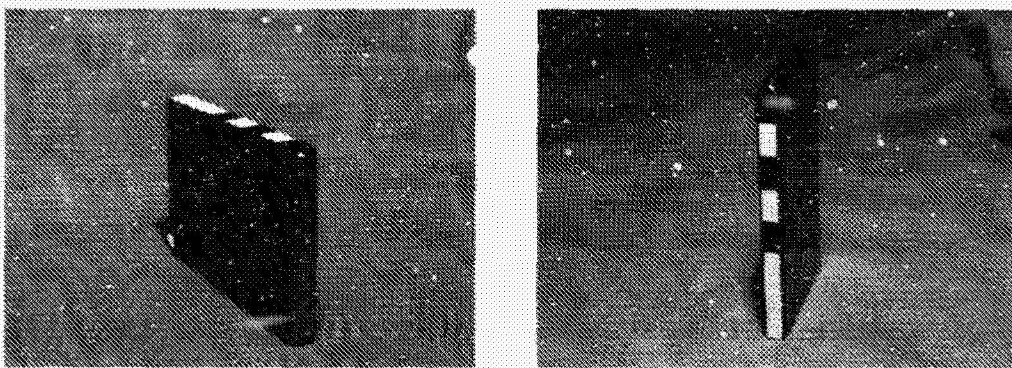

FIGURE 1. 304L STAINLESS STEEL PROJECTILE

The intended projectile velocity was 275 m/sec (900 ft/sec), except in a few tests involving one or two layers of fabric, in which case the impact velocity was approximately 100 m/sec (328 ft/sec). Actual impact velocities were measured using a high-speed digital video camera located above the target.

The gas gun used to accelerate the projectile consisted of a pressure vessel with a volume of 0.35 m^3 (12.5 ft^3), a gun barrel with a length of 12.2 m (40 ft), and an inner diameter of 20.32 cm (8.00 in.). The pressure vessel and the gun barrel were mated by a flange on each side with a number of layers of Mylar® sheets sandwiched between the flanges to seal the pressure vessel and acting as a burst valve. Helium gas was used as the propellant. The pressurized helium was released into the gun barrel by applying a voltage across a Nichrome wire embedded in the Mylar sheets, causing the Mylar sheets to rupture. The projectile was supported in rigid foam inside an aluminum can-shaped cylindrical sabot that just fits inside the gun barrel. The sabot and foam projectile support were stopped at the end of the gun barrel by a thick steel plate with a rectangular slot large enough to allow the projectile to pass through. The gun barrel was evacuated to reduce blast loading on the specimen and to reduce the amount of pressure needed to achieve the desired impact velocity. The gas gun and test setup are shown in figures 2 and 3.

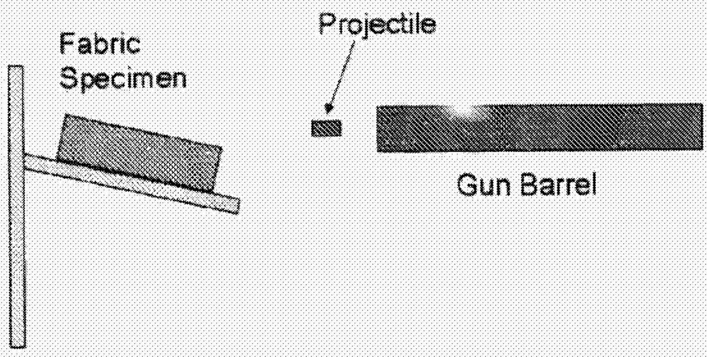

FIGURE 2. SCHEMATIC OF TEST SETUP

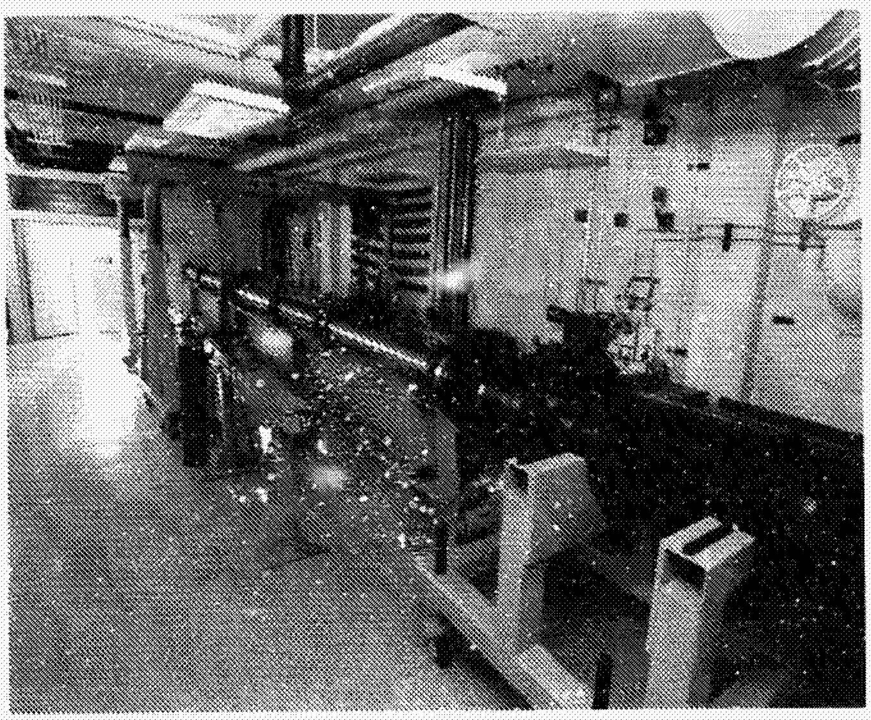

FIGURE 3. GAS GUN USED FOR THE IMPACT TEST

The fixture used to hold the fabric was a 2.5-cm (1-in.)-thick metal ring with a 25 cm (10 in.) height and a diameter of 102 cm (40 in.). A 25-cm (10-in.)-wide fabric strip was rolled around the ring under controlled tension to makeup the desired number of layers. The ring had a 25.4-cm (10-in.) opening and was placed in front of the gun barrel at a 15° incline such that the projectile, after exiting the gun barrel passed over the front edge of the ring, passed through the opening in the fixture and impacted the fabric from the general direction of the center of the ring. The test fixture and specimen are shown in figure 4.

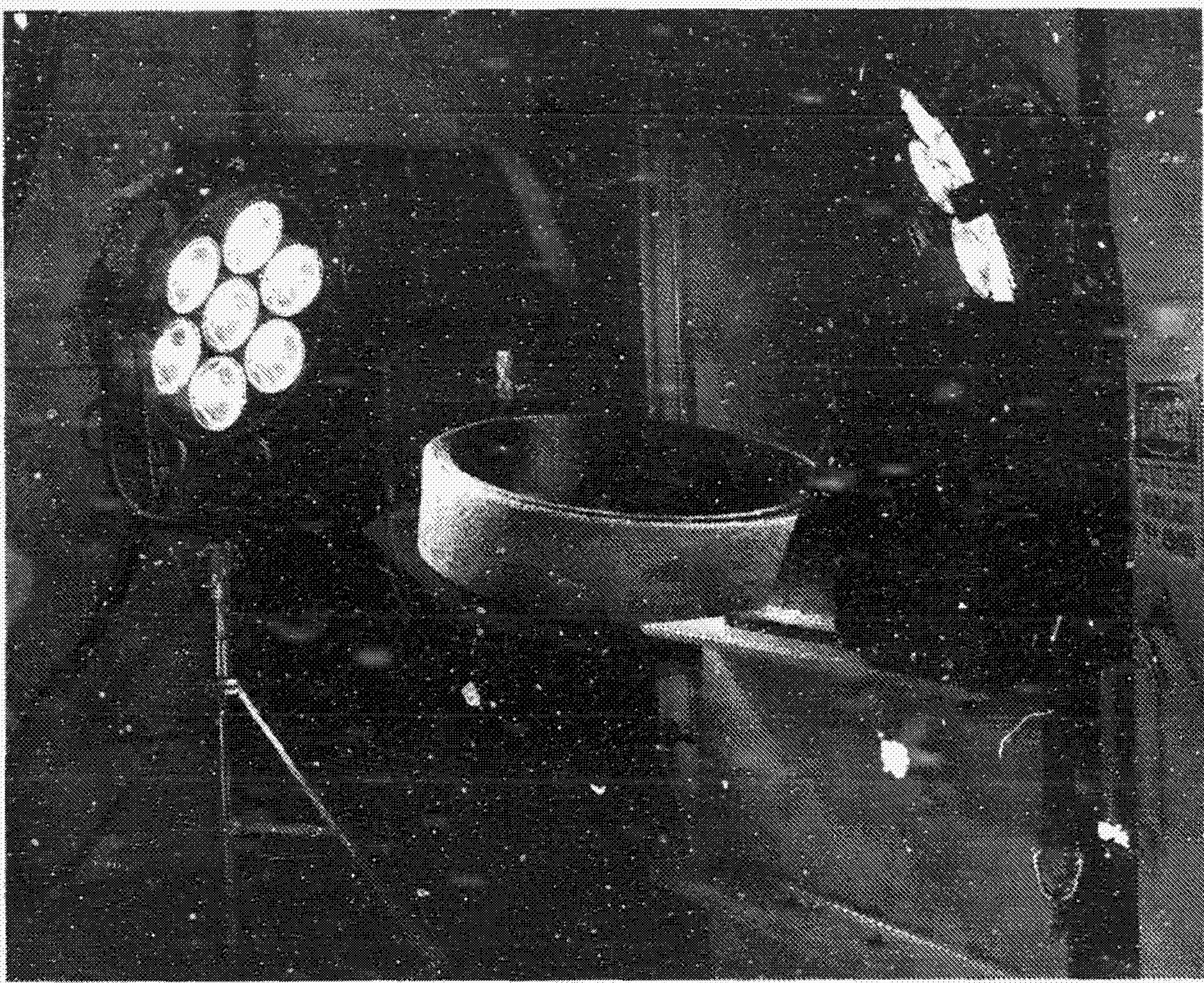

FIGURE 4. TEST FIXTURE WITH KEVLAR SPECIMEN IN PLACE

Each fabric specimen consisted of a continuous 25-cm (10-in.)-wide fabric strip wrapped around the test fixture under controlled tension to produce the desired number of layers. The beginning and end of the continuous strip were held with an epoxy adhesive and were located 180 degrees away from the impact location. The tension in the fabric strip was controlled by placing a fabric spool on the axis of an electric motor with controllable torque, passing the fabric strip around a roller mounted on a load cell and then around the fixture ring (figure 5). The fixture ring was then rotated on bearings while maintaining a torque on the electric motor such that the load cell reading remained constant. The tension in the fabric was controlled to be 24.5 N (5.5 lb).

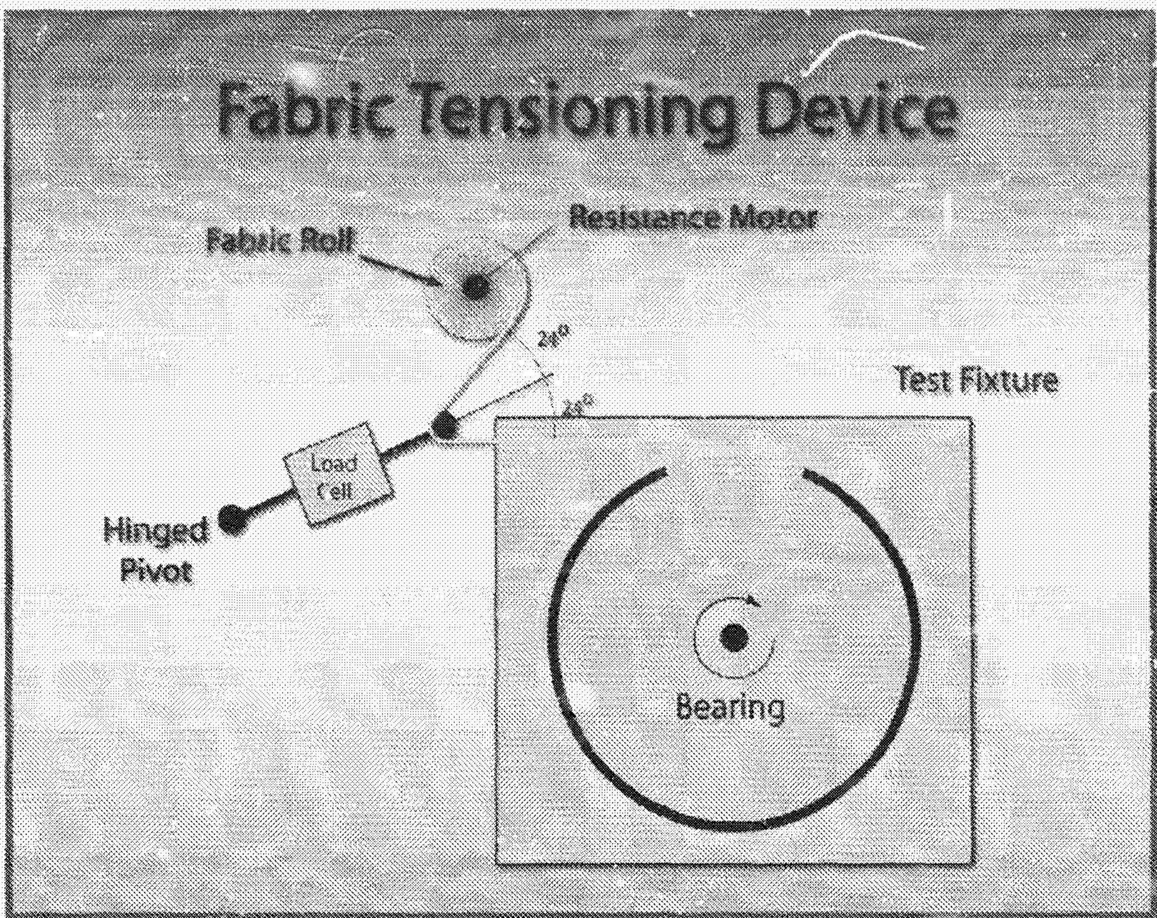

FIGURE 5. SCHEMATIC OF DEVICE USED TO CONTROL TENSION WHILE WINDING THE FABRIC SPECIMEN ON THE FIXTURE

High-speed digital video cameras (Phantom 5, Photosonics Inc., Burbank, CA) were used to record the position and orientation of the projectile during the experiment. The recording speed was 11,200 frames per second, with a 256 by 256 pixel resolution. For a limited number of tests, the recording rate was increased to 38,461 frames per second, with a resolution of 256 by 64 pixels. One camera was located directly above the impact point and the other at an oblique angle. The positions of the cameras are shown in figure 6. A laboratory coordinate system was established, with an origin at the impact point on the fabric (center of the fabric strip), an X axis in the direction of the gun barrel, and a Z axis pointed vertically upward. The upper camera was calibrated to have a scale of 5.610 pixels/cm (14.25 pixels/in.) in the horizontal plane at the top of the projectile and 5.528 pixels/cm (14.04 pixels/in.) in the horizontal plane of the center of the projectile. This calibration applied to both the X and Y directions and for both recording speeds, as the field of view in the Y direction was reduced by a factor of 4 for the higher recording speed.

For each test, the position of two or more points on the projectile was recorded as a function of time. The impact velocity and residual velocity (velocity after perforating the fabric) were determined by fitting a straight line to the position data, while in free flight before and after impact, and averaging the slopes of the resulting lines. In general, the projectile was obscured by the specimen during the impact itself, so it was not possible to obtain accurate enough position data to calculate the projectile deceleration and the resulting force on the projectile during the impact. The fabric deformation at the center of the impact point on the specimen, as viewed by the overhead camera, was also recorded and plotted for each test.

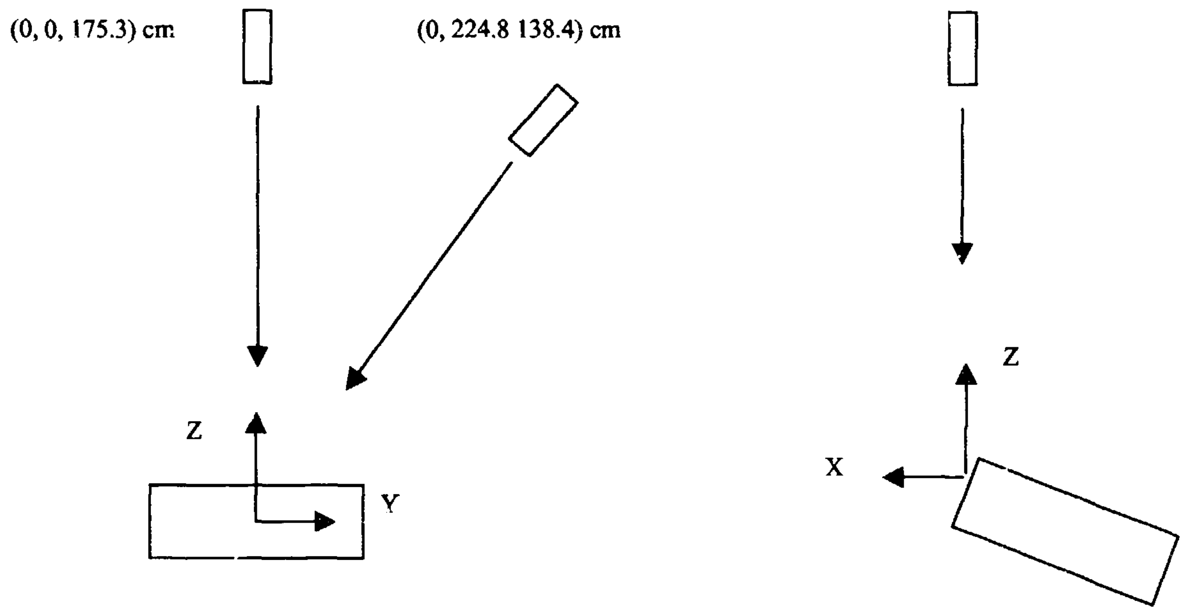

FIGURE 6. SCHEMATIC OF CAMERA LOCATIONS

3. RESULTS AND DISCUSSION.

Twenty-nine impact tests were conducted, fourteen on Kevlar 49, nine on the lighter weight Zylon material and six on the heavier weight Zylon. Figures 7 and 8 show still images taken from typical video data from two tests. Spatial resolution was 256 pixels over a length of approximately 25 cm, or approximately 0.1 cm/pixel. Because of the relatively small amount of motion of the projectile between frames, this resolution could lead to inaccurate velocity measurement if only two frames were used to calculate velocity. Much greater accuracy was possible by fitting a curve to the displacement data over multiple frames.

Tables 2 and 3 summarize the results of the test program. More detailed information on each test, including projectile position as a function of time and fabric deformation, is given in appendix A.

FIGURE 7. SELECTED IMAGES FROM TEST LG407, OBLIQUE VIEW

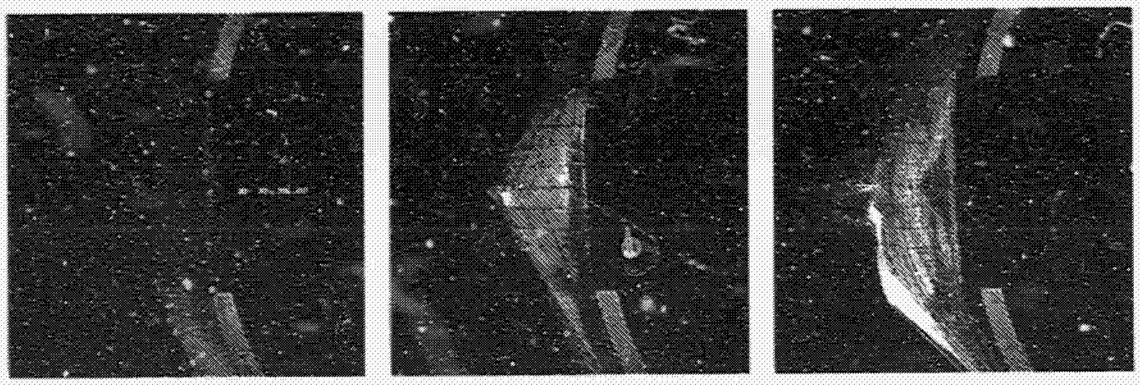

FIGURE 8. SELECTED IMAGES FROM TEST LG420, TOP VIEW

TABLE 2. PROJECTILE IMPACT AND RESIDUAL VELOCITY

Test	Material	Number of Layers	Projectile Mass (g)	Impact Velocity (m/sec)	Exit Velocity (m/sec)
LG403	Kevlar	4	318.4	274	258
LG404	Kevlar	8	317.8	273	250
LG405	Kevlar	24	319.0	274	151
LG409	Kevlar	8	316.0	271	246
LG410	Kevlar	4	316.4	278	264
LG411	Kevlar	24	314.8	270	126
LG424	Kevlar	8	320.9	254	227
LG427	Kevlar	24	317.9	279	185
LG429	Kevlar	16	316.2	279	219
LG432	Kevlar	16	320.0	273	198
LG433	Kevlar	1	316.7	119	112
LG434	Kevlar	1	315.9	117	110
LG444	Kevlar	2	316.4	106	84.7
LG449	Kevlar	2	316.2	105	85.0
LG406	Light Zylon	4	319.5	273	255
LG408	Light Zylon	8	318.0	276	241
LG412	Light Zylon	4	318.4	243	223
LG413	Light Zylon	8	319.9	275	237
LG417	Light Zylon	8	314.6	272	241
LG425	Light Zylon	8	316.6	277	245
LG426	Light Zylon	16	316.8	277	192
LG407	Light Zylon	24	316.1	275	0
LG414	Light Zylon	24	315.9	251	0
LG420	Heavy Zylon	8	316.3	280	191
LG421	Heavy Zylon	8	317.6	262	155
LG422	Heavy Zylon	4	315.8	280	237
LG423	Heavy Zylon	4	315.1	243	192
LG430	Heavy Zylon	12	315.9	279	109
LG428	Heavy Zylon	16	317.9	277	0

TABLE 3. TEST ENERGY AND MAXIMUM DEFLECTION

Test	Impact Kinetic Energy (Joules)	Exit Kinetic Energy (Joules)	Energy Absorbed (Joules)	Approximate Maximum Deflection (cm)
LG403	11980	10560	1419	8.3
LG404	11877	9902	1975	8.9
LG405	11949	3645	8303	11.4
LG409	11561	9583	1978	8.3
LG410	12224	10996	1227	7.6
LG411	11478	2494	8984	12.7
LG424	10368	8251	2117	8.3
LG427	12363	5458	6904	8.9
LG429	12270	7614	4656	8.9
LG432	11933	6280	5653	10.2
LG433	2226	1981	244	
LG434	2163	1912	251	
LG444	1790	1135	654	
LG449	1748	1143	604	
LG406	11888	10347	1540	10.2
LG408	12071	9265	2805	11.4
LG412	9418	7946	1471	12.1
LG413	12063	8948	3115	11.4
LG417	11627	9143	2484	11.4
LG425	12125	9506	2618	10.8
LG426	12159	5859	6300	12.7
LG407	11946	0	11946	
LG414	9939	0	9939	
LG420	12354	5739	6615	12.7
LG421	10886	3807	7078	11.4
LG422	12335	8833	3501	10.8
LG423	9320	5790	3529	11.4
LG430	12312	1859	10452	14.0
LG428	12174	0	12174	

In all tests, except tests LG407, LG414, and LG428, the projectile perforated the fabric specimen. The failure was generally along the line defined by the leading edge of the projectile. In the initial plies, the failure was highly localized along this line. and to the naked eye resembled a cut in the fabric. As the projectile progressed through the layers, the failure point remained generally along the same line, but there was significant fraying at the ends of the failed yarns. The fraying is indicative of individual fibers within the yarn failing at different locations. The same phenomena existed in cases where full perforation did not occur. In these cases, it was clear that failure initiated at the corners of the projectile. There were several plies where there were holes at the corner locations while the material in between remained intact. Progressing from the outer layers to the inner layers, the holes grew in size until there was failure across the total leading-edge region.

The impact, exit and absorbed kinetic energy, shown in table 3, were calculated from the mass and velocity of the projectile before and after perforation. As shown in table 2, in all but three tests, the projectile perforated the fabric specimen. Figure 9 shows the energy absorbed as a function of the number of fabric layers in each test. The arrows on selected symbols indicate that in these tests the projectile did not penetrate the specimen (all of the kinetic energy was absorbed) and more energy could have been absorbed. The lines in the figure are quadratic curve fits to the data. Figure 10 shows the same data but the energy is normalized by the areal mass of each specimen. The areal mass of the specimen is defined as the areal mass per layer, in grams per square centimeter, times the number of layers.

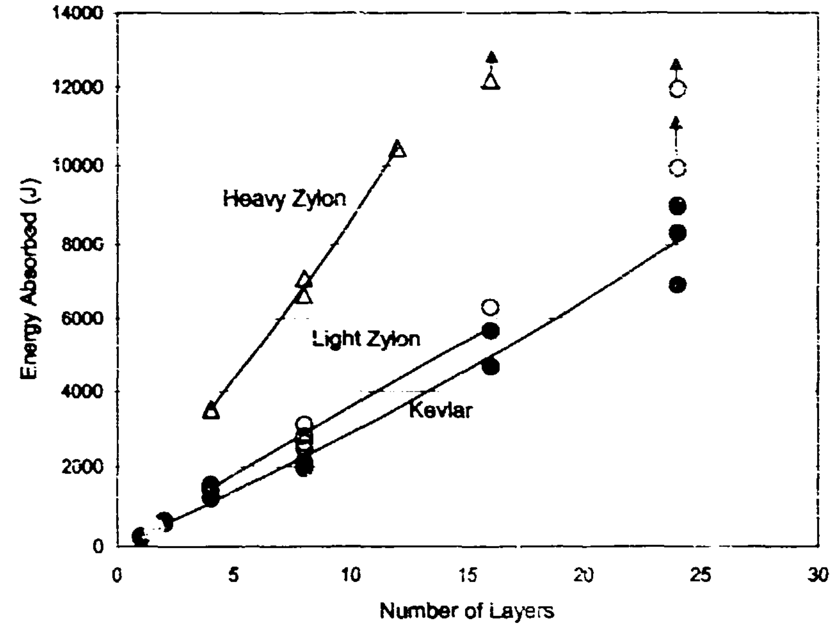

FIGURE 9. ENERGY ABSORBED AS A FUNCTION OF NUMBER OF FABRIC LAYERS

It is clear from figures 9 and 10 that for a given weight and under these impact conditions, Zylon is able to absorb significantly more energy than Kevlar, and the heavier Zylon is more effective than the lighter version of the same material. The heavier weight Zylon and the Kevlar material were very similar in areal weight, fiber count, ply thickness, and yarn denier. Figure 10 illustrates that the normalized absorbed energy is relatively insensitive to the number of layers of material. For the Kevlar material, the average normalized absorbed energy is 13.5 kJ-g/cm^2. For the lighter weight Zylon, this value is 22.9 kJ-g/cm^2, and for the heavier weight Zylon, the value is 38.9 kJ-g/cm^2. From a practical point of view, this means that for the same weight of material, the thick Zylon can absorb almost three times as much energy than the Kevlar material under the conditions of this test.

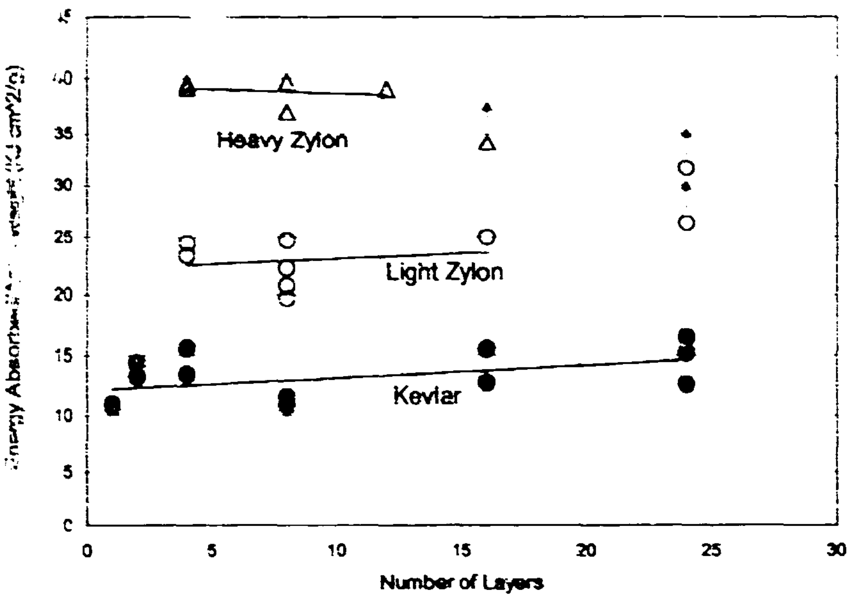

FIGURE 10. NORMALIZED ENERGY ABSORBED AS A FUNCTION OF NUMBER OF FABRIC LAYERS

The two data points for the lighter weight Zylon corresponding to tests where the projectile did not perforate the fabric indicate that if perforation occurs, there is less energy absorbed than the specimen is capable of absorbing when perforation does not occur. This is consistent with data in the literature for fabric materials where it has been shown that, typically, as the impact energy is increased until perforation occurs, a plot of absorbed energy as a function of impact velocity will show a sudden decrease after the ballistic limit velocity is exceeded [18]. Beyond this point, the absorbed energy may increase, decrease, or remain constant.

The maximum deflection in the fabric was determined from plots of the fabric deformation shown in appendix A. Because of the progressive nature of failure in the specimen, once failure initiated, the shape of the fabric was difficult to accurately measure. Therefore, the maximum deflection in the fabric is accurate only to within approximately 0.5 cm. The maximum deflection in the fabric during the test is shown in figure 11.

The figure shows a significant amount of scatter. Some of this is attributed to the difficulty in obtaining an accurate measurement of the maximum deflection. Despite the scatter, there is a definite trend in the data. The deflection data falls into three general ranges of normalized energy absorbed corresponding to the three different specimen types. The figure illustrates that the difference in maximum deflection is greater between Kevlar and 500-denier Zylon than that between the lighter and heavier Zylon. The increase in maximum normalized absorbed energy between the two different weight Zylon specimens is relatively large, while the increase in maximum deflection is moderate.

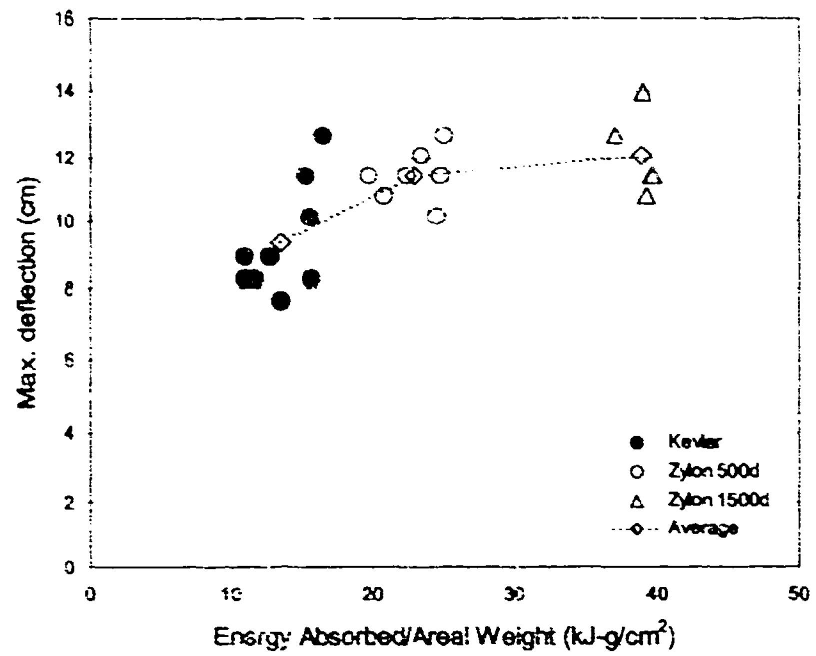

FIGURE 11. MAXIMUM DEFLECTION IN FABRIC
(The maximum deflection occurred just prior to full perforation if the projectile perforated the fabric.)

4. CONCLUDING REMARKS.

In this study, ballistic impact tests were conducted at National Aeronautics and Space Administration Glenn Research Center on dry Kevlar 49 and Zylon AS fabric specimens in a test configuration designed to simulate its application in a turbine engine fan containment system.

The test configuration described herein was designed to be somewhat representative of fabric containment systems used in jet engines, while maintaining repeatability and simplicity in the test. The data obtained from these tests were used to develop improved computational models or fabric containment systems. The results show that under the conditions of this test, Zylon is able to absorb almost three times as much energy than Kevlar when compared on an overall weight basis. The normalized energy absorbed is relatively insensitive to the number of layers of material. This allows for a fairly simple design procedure if the assumption is made that the amount of energy absorbed per unit weight is independent of the number of layers of material. Under the conditions of this test, the heavier weight Zylon material performed better than the lighter weight material, for the same overall weight.

5. REFERENCES.

1. Federal Aviation Administration, Title 14 Code of Federal Regulations 33.94, 1984.

2. "LS-DYNA Theoretical Manual," Livermore Software Technology Corp., Livermore, CA, 1998.

3. "ABAQUS/Explicit User's Manual," ABAQUS, Inc., Pawtucket, RI, 2003.

4. Wong, A.K and Connors, M.L., "A Literature Survey on Correlation of Laboratory Tests and the Ballistic Resistance of Rolled Homogeneous Stell and Aluminum Armors," Technical Report AMMRC SP 72-10, Army Materials and Mechanics Research Center, Watertown, MA, September 1971.

5. Clifton, R.J., "Response of Materials Under Dynamic Loading," *International Journal of Solids and Structures*, Vol., 37, 2000, pp. 105-113.

6. Johnson, G.R. and Cook, W.H., "Fracture Characteristics of Three Metals Subjected to Various Strains, Strain Rates, Temperatures and Pressures," *Engineering Fracture Mechanics*, Vol. 21(1), 1985, pp. 31-48.

7. Roylance, D. and Wang, S.S., "Penetration Mechanics of Textile Structures in Ballistic Materials and Penetration Mechanics," R.C. Laible, ed., Elsevier, 1980.

8. Cunniff, P.M., "A Semi-Empirical Model for the Ballistic Impact Performance of Textile-based Personnel Armor," *Textile Research Journal*, Vol. 56, 1996, pp. 45-60.

9. Figucia, F., "Energy Absorption of Kevlar Fabrics Under Ballistic Impact," Technical Report A090390, Defense Technical Information Center, 1980.

10. Tabiei, A. and Ivanov, I., "Computational Micro-Mechanical Model of Flexible Woven Fabric for Finite Element Impact Simulation," *International Journal of Numer. Meth., Engng*, Vol. 53, 2002, pp. 1259-1276.

11. Lim, C.T., Shim, V.P.W., and Ng, Y.H., "Finite-Element Modeling of the Ballistic Impact of Fabric Armor," *International Journal of Impact Engineering*, Vol. 28, 2003, pp. 13-31.

12. Zohdi, T.I., "Modeling and Simulation of Progressive Penetration of Multilayered Ballistic Fabric Shielding," *Comput. Mech.*, Vol. 29(1), 2002, pp. 61-67.

13. Scala, P.E., "A Brief History of Composites in the U.S.—The Dream and the Success," *JOM*, Vol. 48 (2), 1996, pp. 45-48.

14. Stotler, C.L., "Development of Advanced Lightweight Containment Systems," NASA CR-165212, National Aeronautics and Space Administration, 1981.

15. Shockey, D.A., Erlich, D.C., and Simons, J.W., "Lightweight Fragment Barriers for Commercial Aircraft," *18th International Symposium on Ballistics*, San Antonio, TX, 15-19 November 1999.

16. Pereira, J.M., Roberts, G.D., and Revilock, D.M., "Elevated Temperature Ballistic Impact Testing of PBO and Kevlar Fabrics for Application in Supersonic Jet Engine Fan Containment Systems," NASA TM-107532, August 1997.

17. Simons, J.W., Erlich, D.C., and Shockey, D.A., "Explicit Finite Element Modeling of Multi-layer Composite Fabric for Gas Turbine Engine Containment Systems, Part 3: Model Development and Simulation Experiments." FAA report DOT/FAA/AR-04/40,P3, November 2004.

18. Cunniff, P.M., "An Analysis of the System Effects in Woven Fabrics Under Ballistic Impact," *Textile Research Journal*, 62 (9), 1992.

APPENDIX A—FABRIC DEFORMATION

The following graphs display the deformation of the fabric in a horizontal plane passing through the center of the impact point. The deflection is plotted as a sequence of curves measured from the camera video images.

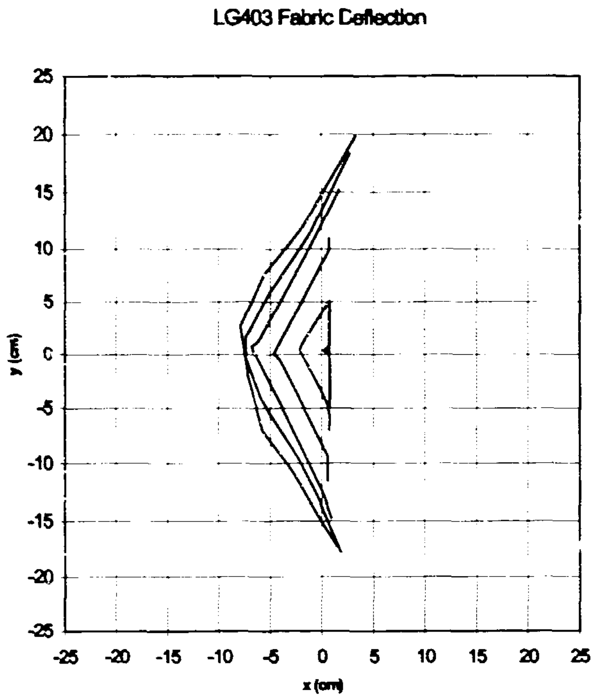

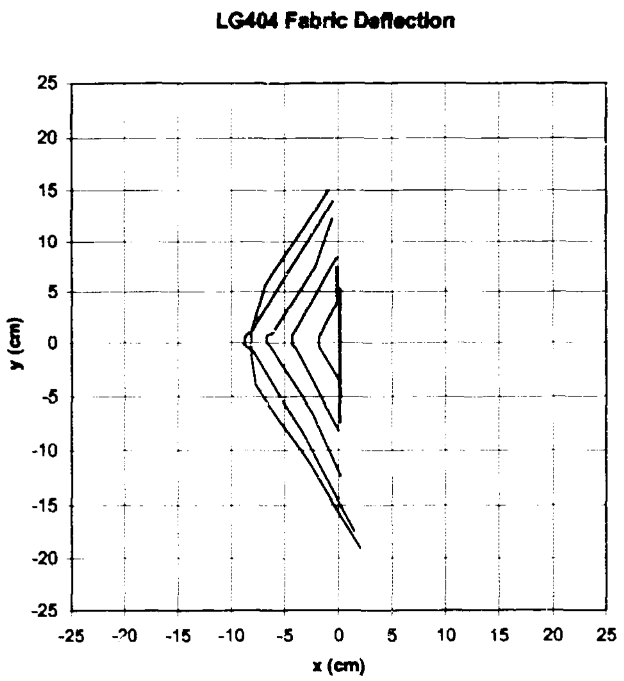

LG405 Fabric Deflection

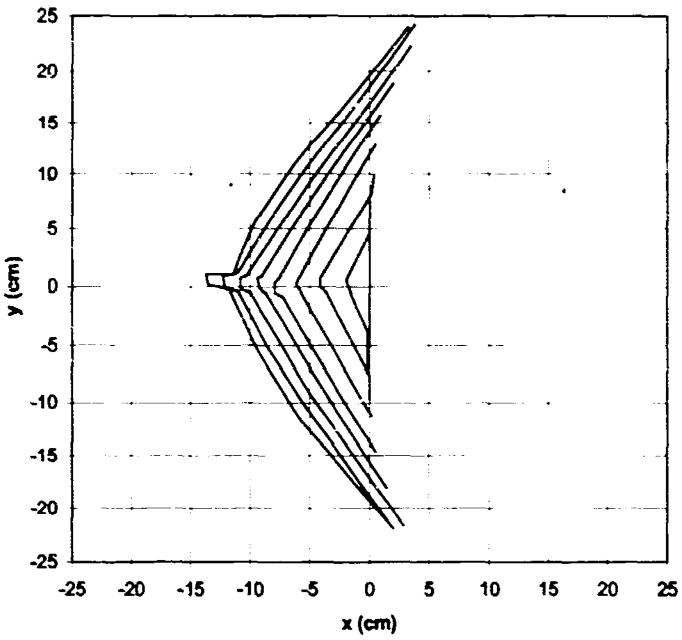

LG406 Fabric Deflection

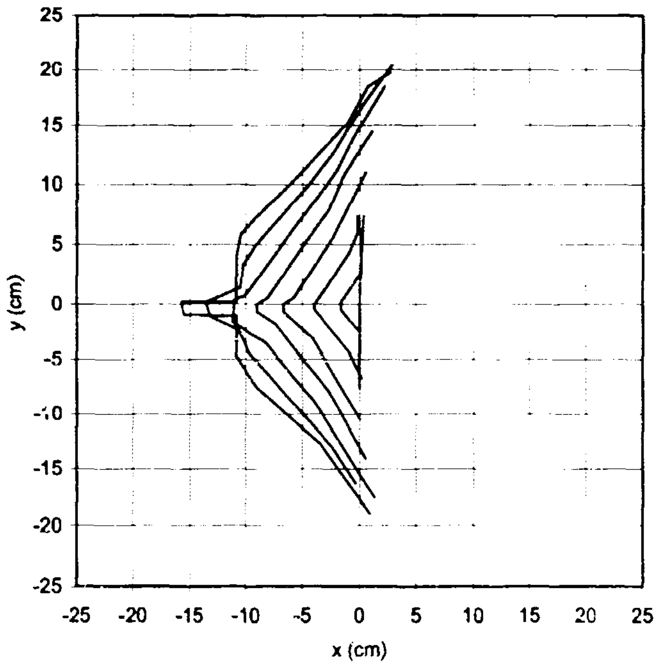

LG407 Fabric Deflection

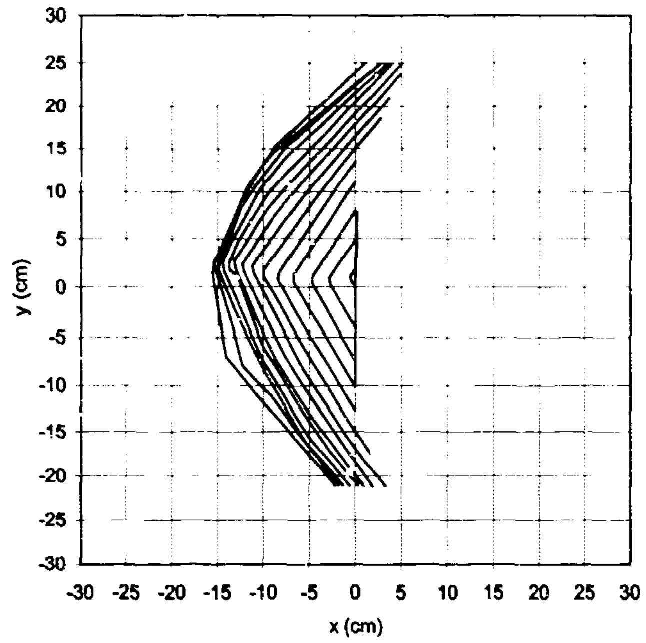

LG408 Fabnc Deflection

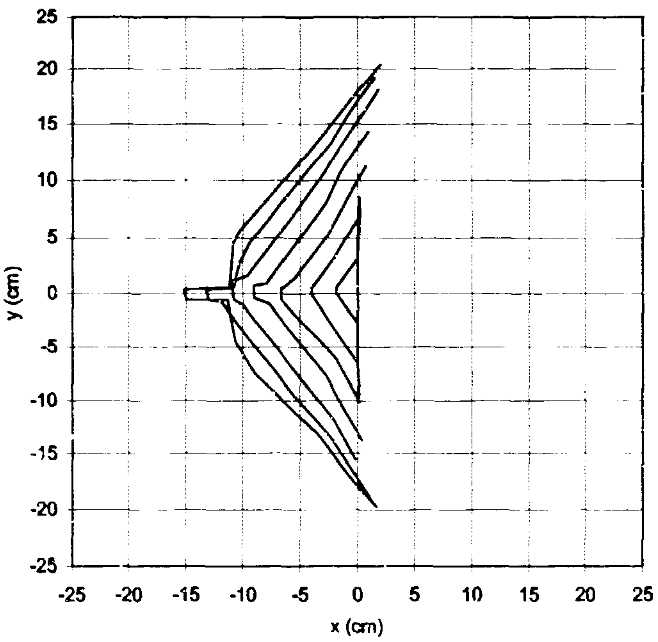

LG409 Fabric Deflection

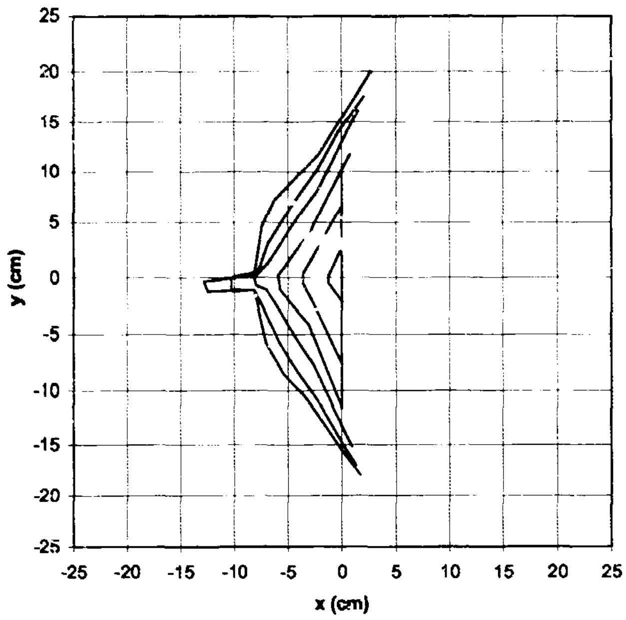

LG410 Fabric Deflection

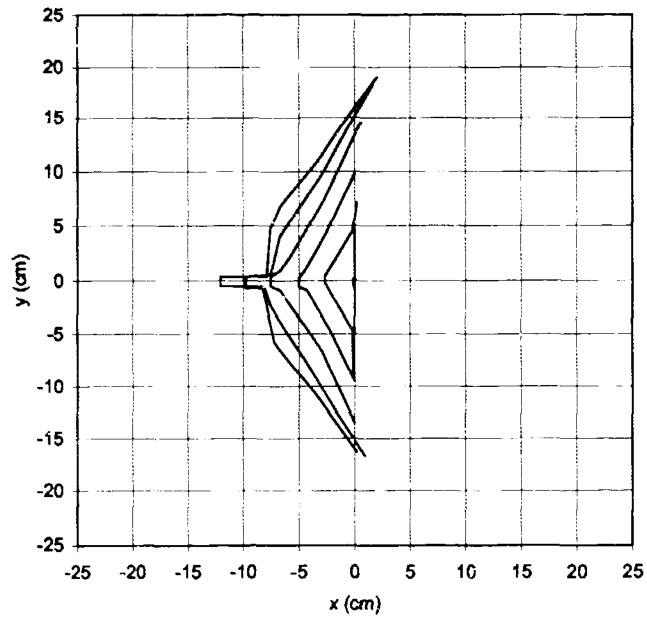

LG411 Fabric Deflection

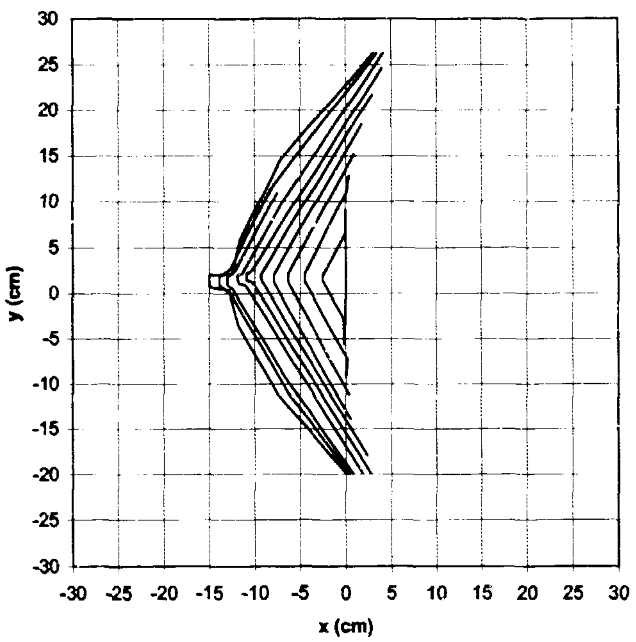

LG412 Fabric Deflection

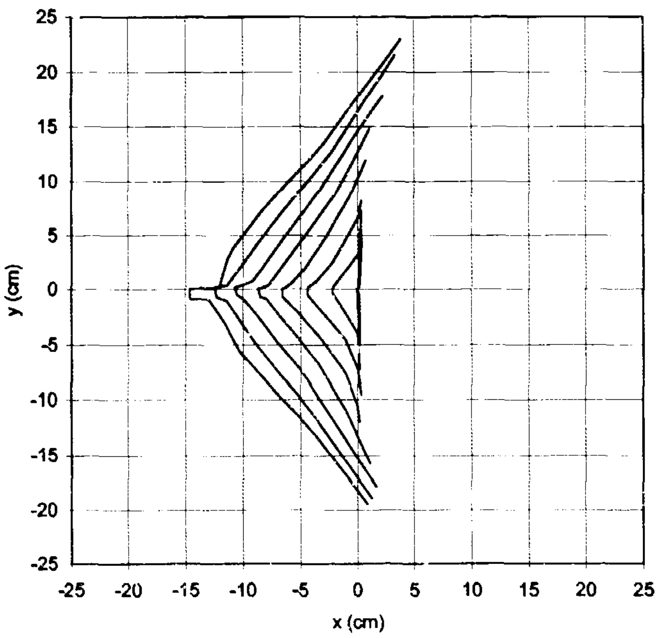

LG413 Fabric Deflection

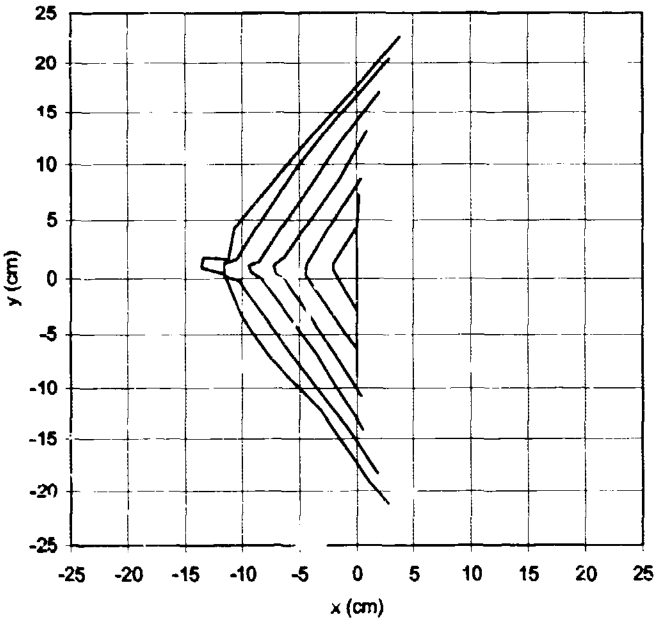

LG414 Fabric Deflection

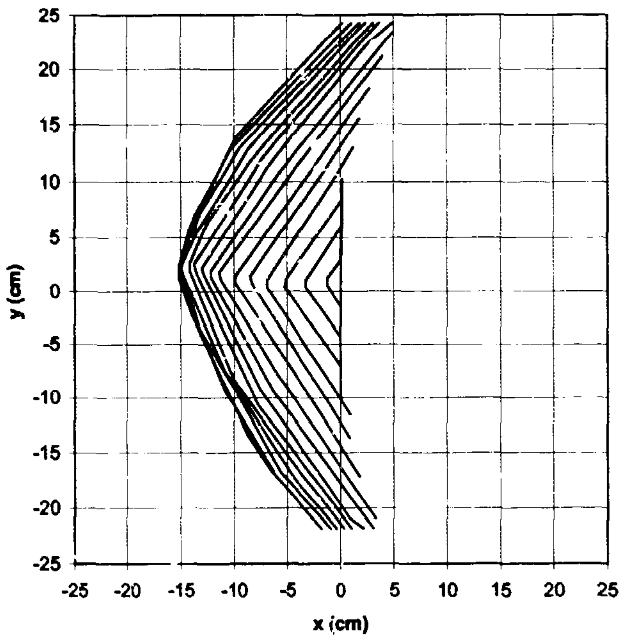

LG417 Fabric Deflection

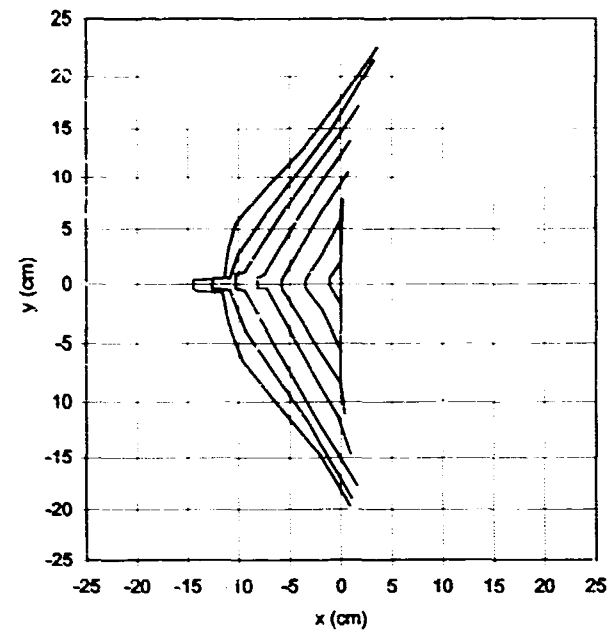

LG420 Fabric Deflection

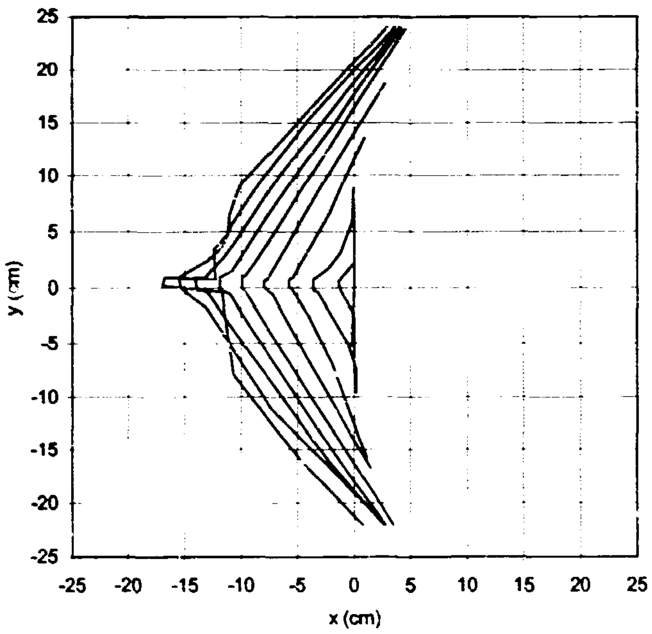

LG421 Fabric Deflection

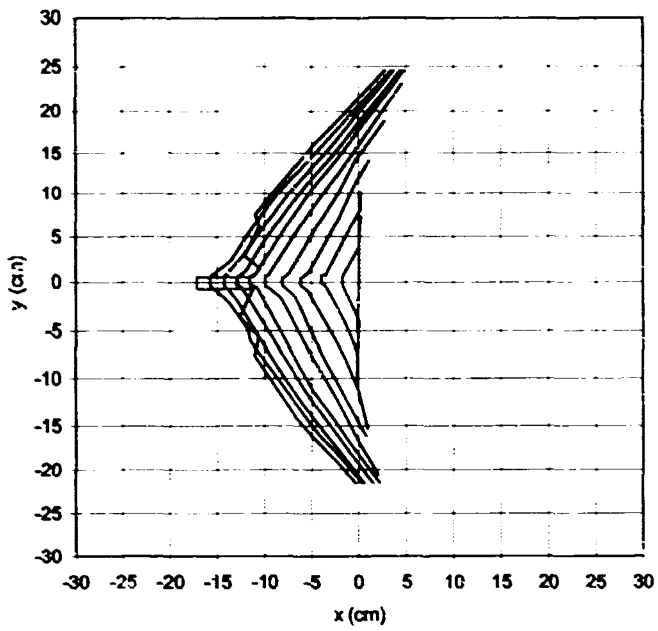

LG422 Fabric Deflection

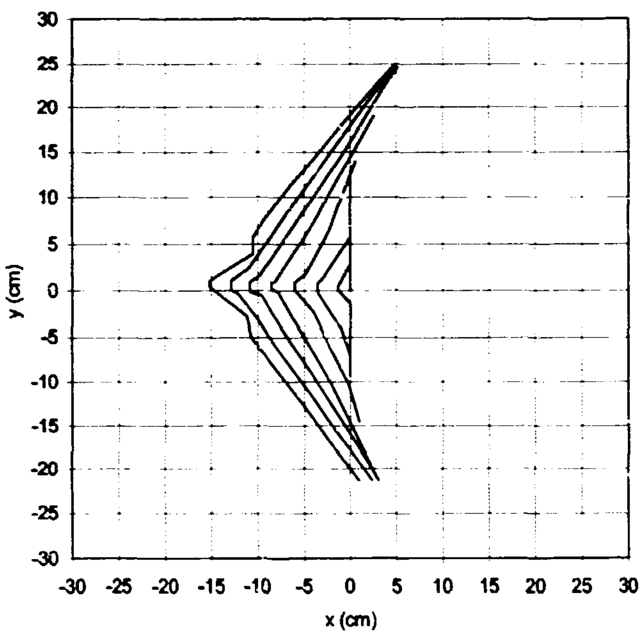

LG423 Fabric Deflection

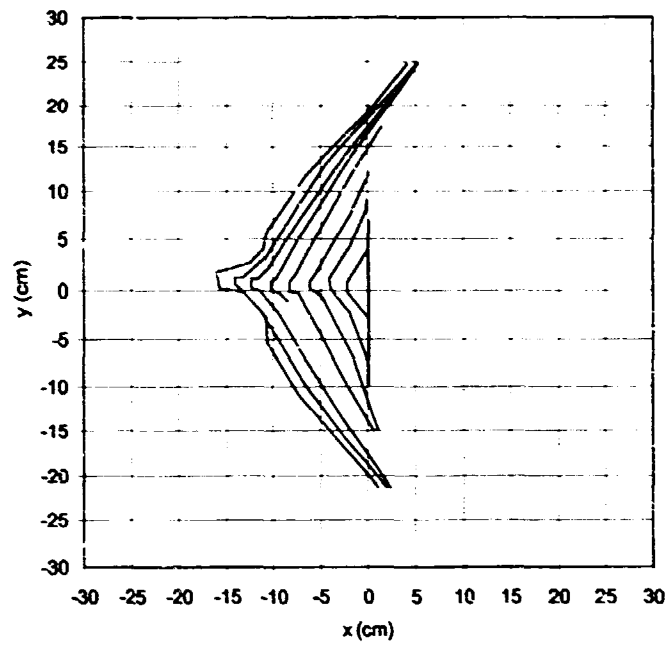

LG424 Fabric Deflection

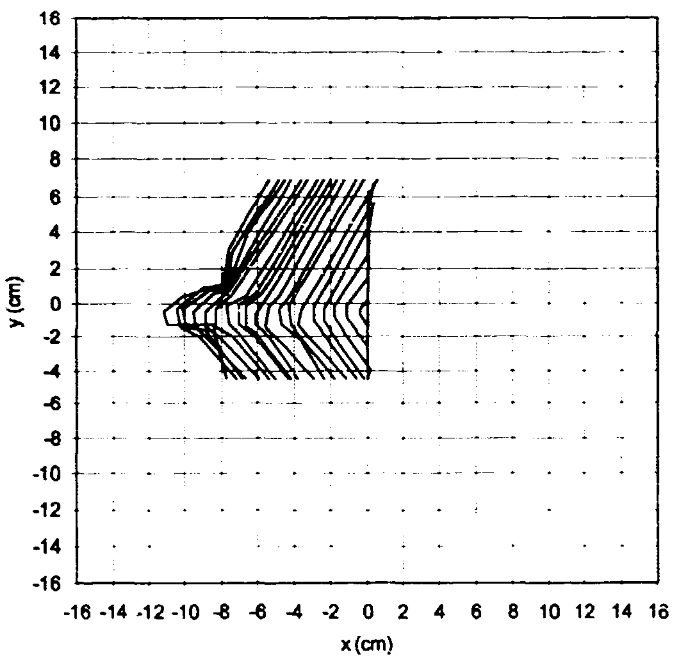

LG425 Fabric Deflection

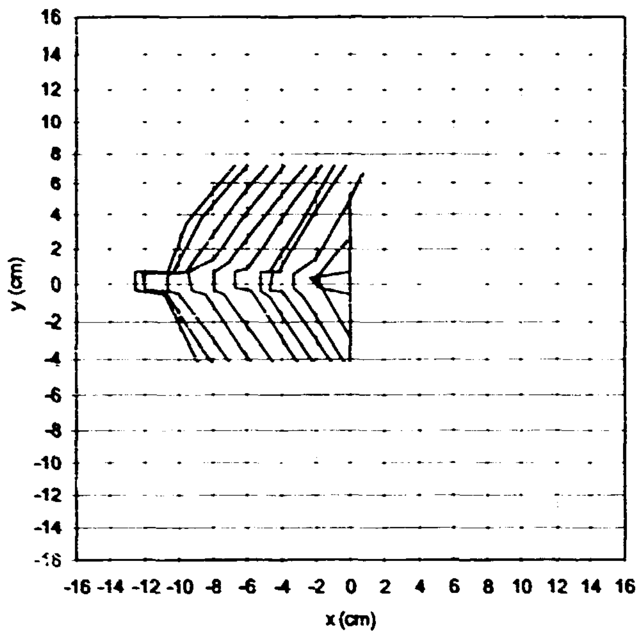

LG426 Fabric Deflection

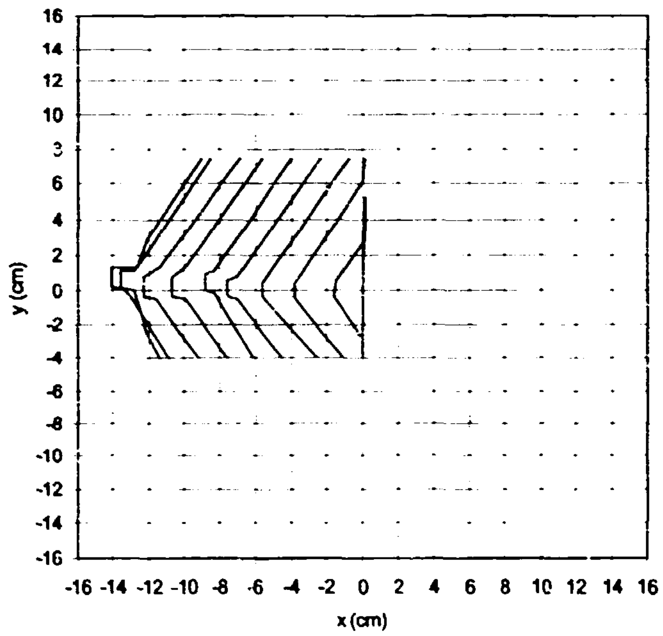

LG427 Fabric Deflection

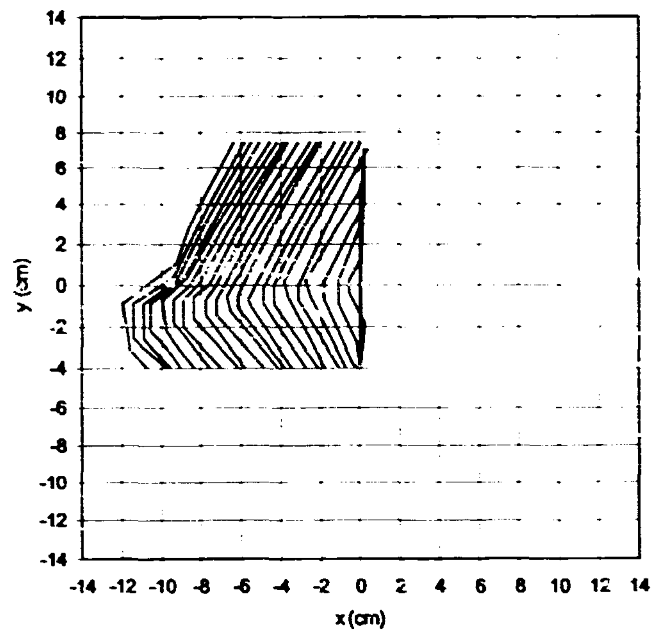

LG428 Fabric Deflection

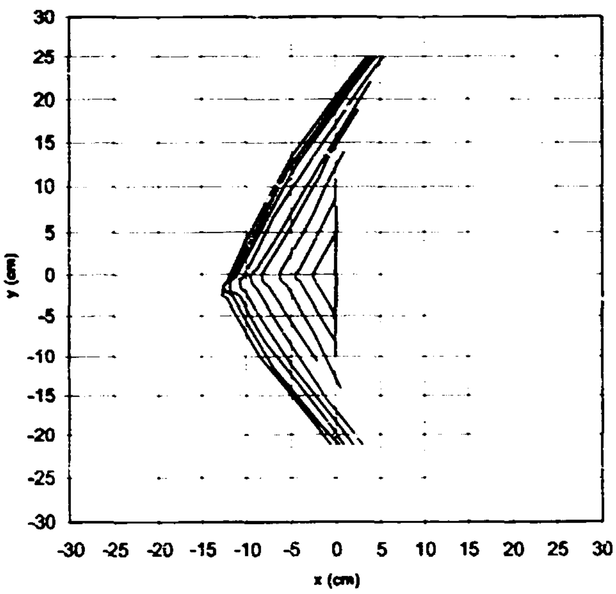

LG429 Fabric Deflection

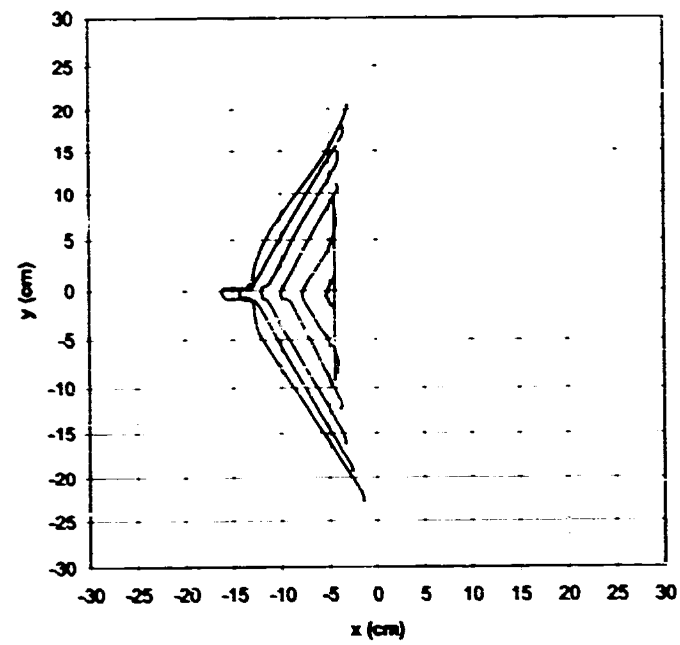

LG430 Fabric Deflection

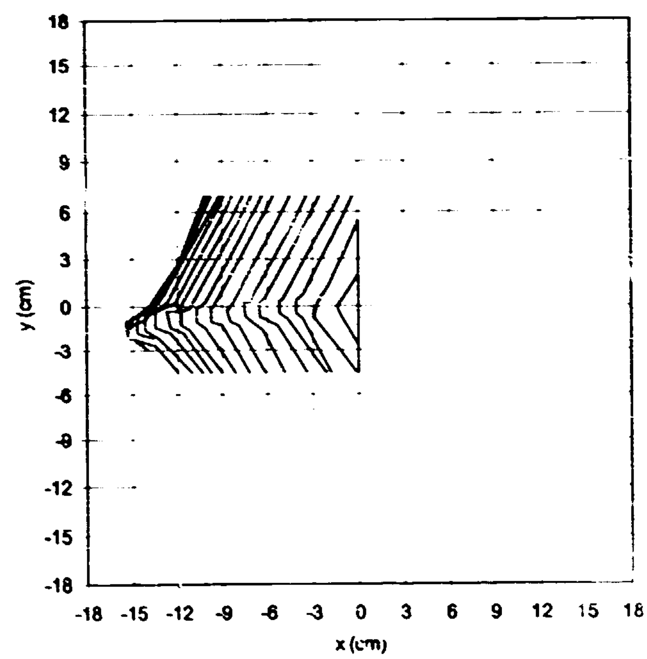

LG432 Fabric Deflection

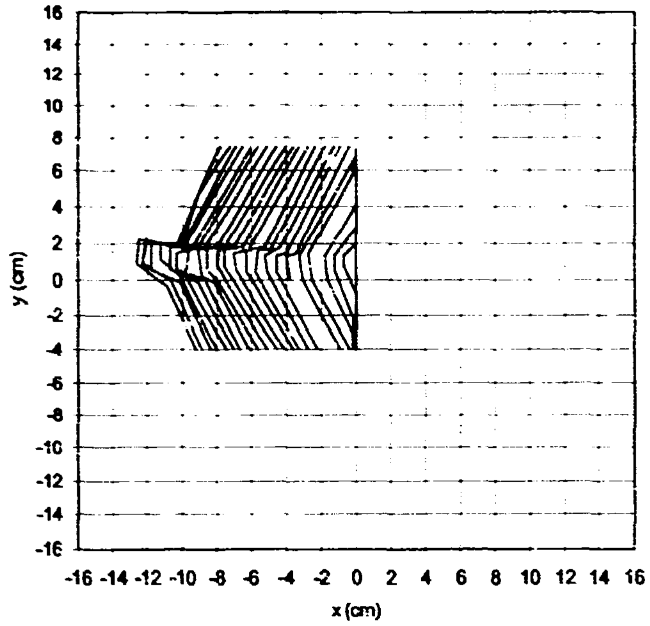

LG433 Fabric Deflection

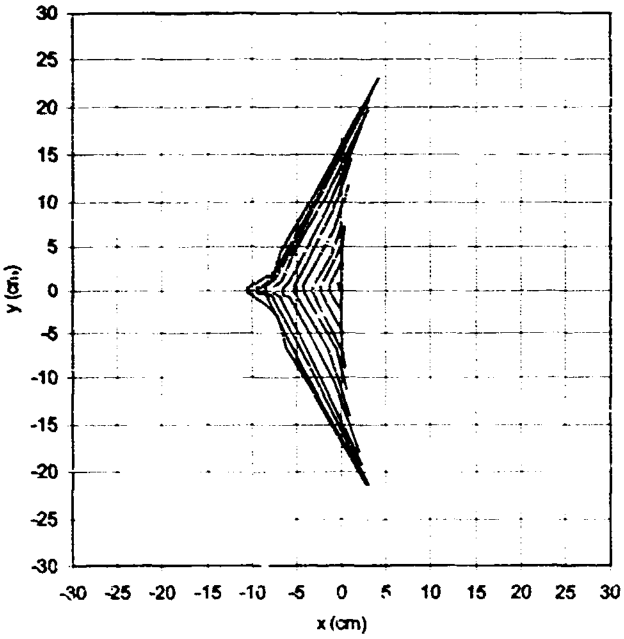

LG434 Fabric Deflection

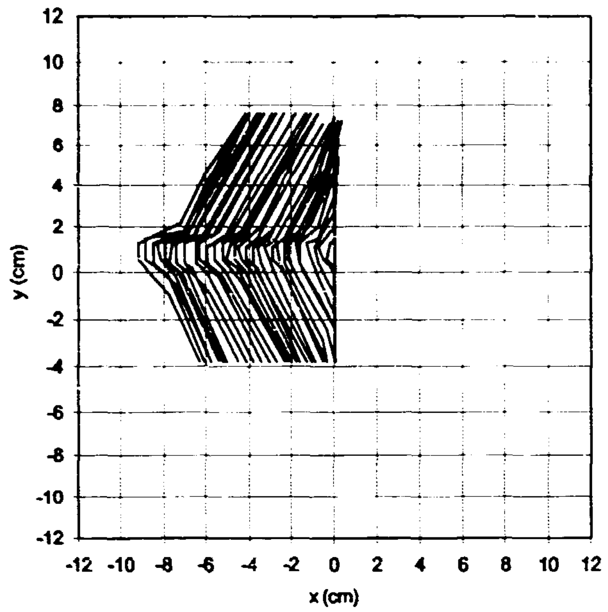

LG444 Fabric Deflection